ORIGINAL ARTICLE

Optimized lesion size index (o-LSI): A novel predictor for sufficient ablation of pulmonary vein isolation

Gen Matsuura MD [iD] | Jun Kishihara MD, PhD [iD] | Hidehira Fukaya MD, PhD [iD] |
Jun Oikawa MD, PhD | Naruya Ishizue MD, PhD | Daiki Saito MD | Tetsuro Sato MD |
Yuki Arakawa MD | Shuhei Kobayashi MD | Yuki Shirakawa MD | Ryo Nishinarita MD [iD] |
Ai Horiguchi MD | Shinichi Niwano MD, PhD [iD] | Junya Ako MD, PhD

Department of Cardiovascular Medicine, Kitasato University School of Medicine, Sagamihara, Kanagawa, Japan

Correspondence
Jun Kishihara, MD, PhD, Department of Cardiovascular Medicine, Kitasato University School of Medicine, 1-15-1 Kitasato, Minami-ku, Sagamihara 252-0374, Japan.
Email: j_kishihara@med.kitasato-u.ac.jp

Abstract

Background: Although the lesion size index (LSI) has been well established, it is sometimes difficult to achieve first-pass pulmonary vein isolation (PVI) and to avoid acute pulmonary vein reconnections, even with LSI-guided procedures. The purpose of this study was to assess the predictive accuracy of a novel parameter, the optimized lesion size index (o-LSI), to perform PVI.

Methods: The voltage maps created by the Advisor™ high-density (HD) grid catheter before PVI in 35 atrial fibrillation (AF) patients were examined for an association between the voltage amplitude and insufficient ablation sites (IAS), which were defined as either (i) spontaneous reconnection sites, (ii) dormant PV conduction sites unmasked with 20 mg of adenosine triphosphate disodium hydrate (ATP) injection, or (iii) PV-LA gap sites after the initial PVI.

Results: IAS was observed in 25/1417 of the total ablation sites. IAS was significantly associated with higher bipolar voltage areas (4.20 ± 2.68 vs 2.43 ± 1.93 mV, $P < .0001$) but not with LSI. A novel index, o-LSI (defined as LSI/bipolar voltage), was significantly lower in IAS than in others (1.14 [0.82, 1.81] vs 2.35 [1.31, 4.80] LSI/mV). By receiver operating characteristic analysis, an o-LSI of 2.04 was the best cutoff value for the prediction of IAS (88% sensitivity and 55% specificity, $P < .0001$, areas under the curve: 0.742).

Conclusion: Low o-LSI was strongly associated with IAS, potentially providing a novel index to improve first-pass PV isolation.

KEYWORDS
atrial fibrillation, high-voltage zone, insufficient ablation sites, lesion size index, pulmonary vein isolation

1 | INTRODUCTION

Pulmonary vein isolation (PVI) is an established treatment for atrial fibrillation (AF).[1-3] Creating durable transmural radiofrequency (RF) lesions and avoiding PV reconnections are quite important for the success rate of AF ablation. The lesion size index (LSI) is a novel multiparametric index that incorporates time, power, contact force (CF), and impedance data recorded during RF ablation in a weighted formula that describes ablation biophysics.[4,5] It predicts RF lesion width and depth of myocardial tissue more accurately than force time integral (FTI), and LSI-guided PVI in patients with AF can improve clinical outcomes compared with non-LSI-guided PVI.[6] Although the optimal LSI for successful PVI has been reported, in clinical practice, it is sometimes difficult to achieve first-pass PVI and to avoid acute pulmonary vein reconnections, even with the LSI-guided procedure. Nagashima et al previously reported that high-voltage zones (HVZs), which were defined by a Pentaray mapping catheter™ (Pentaray NAV; Biosense Webster) within the PV-encircling lines, were a major determinant of acute PV reconnections after PVI because HVZ might reflect a thickened wall or non-diseased cardiomyocytes impeding the creation of a transmural lesion.[7,8] The Advisor™ high-density (HD) grid catheter (Abbott, St. Paul, MN, USA) was created with equispaced multipolar grid electrodes with known bipole spacing in orthogonal directions, thereby providing the ability to discriminate voltage differences in two directions for enhanced directionality and amplitude detection. Based on this structural feature, the Advisor™ HD Grid catheter is expected to create more accurate voltage mapping. We defined the optimized LSI (o-LSI) calculated as LSI/bipolar voltage, which was defined by the Advisor™ HD Grid catheter as the combination of two parameters. The purpose of this study was to assess the predictive accuracy of this novel parameter to perform PVI.
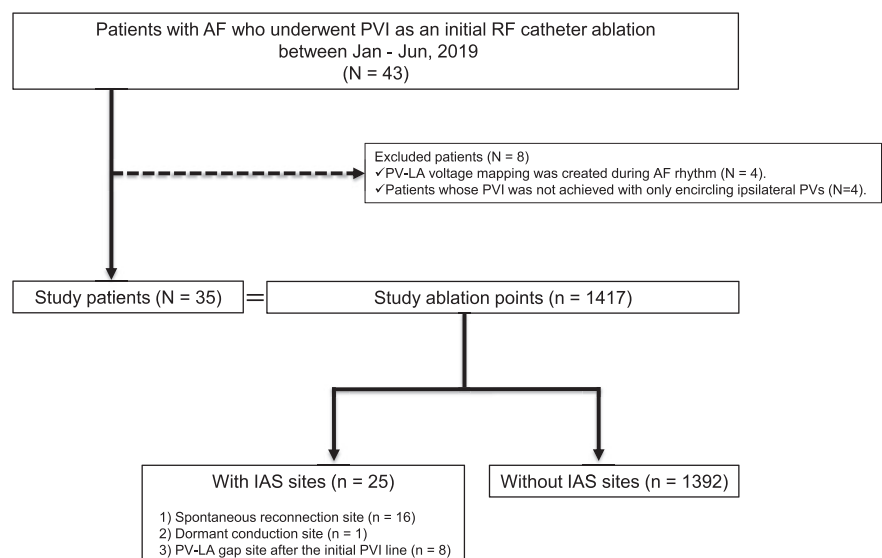
2 | METHODS

2.1 | Study design

This study was a retrospective single-center study that enrolled 35 patients (29 men; mean age 67 ± 9 years) with nonvalvular AF who underwent PVI as an initial RF catheter ablation at our institute between January 2019 and June 2019. The exclusion criteria for this study were as follows: (i) patients could not be converted to sinus rhythm using an intracardiac defibrillator; therefore, HD PV-LA voltage mapping was created during AF rhythm. (ii) For patients whose PVI was not achieved with only encircling ipsilateral PVs, RF application at the carina was required. The flow chart of this study design and outcome is shown in Figure 1. This study complied with the Declaration of Helsinki and was approved by the institutional ethics committee of the hospital of the Kitasato University School of Medicine (approval number B19-217).

2.2 | Catheter setup and voltage mapping

All antiarrhythmic drugs were discontinued for at least 2 days before the electrophysiologic study. The procedure was performed under general anesthesia with propofol, dexmedetomidine, and fentanyl. A multielectrode catheter (BeeAT; Japan Lifeline, Tokyo, Japan) was inserted through the jugular vein and positioned in the coronary sinus. A 9 Fr intracardiac echocardiography catheter (ViewFlex; St Jude Medical) was used for guidance of transseptal puncture. After a single transseptal puncture was performed, unfractionated heparin was intravenously administered to maintain an activated clotting time of >300 seconds. A nonsteerable sheath (Swartz Braided Transseptal Guiding Introducer SL0; Abbott, St. Paul, MN, USA) and a steerable sheath (Agilis; Abbott) were placed into the LA. The 3D geometry of the LA and PVs was created with the use of the EnSite

FIGURE 1 Flow chart of the study design and outcome. All patients were evaluated in accordance with the exclusion criteria. We evaluated 35 patients and 1417 ablation points and divided them into two groups, with or without insufficient ablation sites. IAS was observed at 25 points/1417 of the total ablation sites. Spontaneous PV reconnection was observed at 16 points, ATP-provoked dormant PV conduction at 1 point, and the PV-LA gap site after the initial PVI at 8 points. IAS, insufficient ablation sites; PVI, pulmonary vein isolation; LA, left atrium ATP; adenosine triphosphate disodium hydrate

Patients with AF who underwent PVI as an initial RF catheter ablation between Jan - Jun, 2019 (N = 43)

Excluded patients (N = 8)
✓ PV-LA voltage mapping was created during AF rhythm (N = 4).
✓ Patients whose PVI was not achieved with only encircling ipsilateral PVs (N=4).

Study patients (N = 35) = Study ablation points (n = 1417)

With IAS sites (n = 25)
1) Spontaneous reconnection site (n = 16)
2) Dormant conduction site (n = 1)
3) PV-LA gap site after the initial PVI line (n = 8)

Without IAS sites (n = 1392)

mapping system. After all patients were converted to sinus rhythm using an intracardiac defibrillator, HD PV-LA voltage mapping was created under the constant pacing from right atrium with the Advisor™ HD Grid catheter (Abbott), which has 16×1 mm diameter electrodes with equidistant interelectrode spacing both along and across the splines (center to center, 3 mm), and its mapping system (EnSite Precision) includes a recording device (HD wave solution) that can record 32 bipolar signals (16 along the splines and 16 across the splines). Bipolar high-pass filtering was set at 30 Hz, low-pass filtering was set at 300 Hz, and the noise filter was switched on. Unipolar high-pass filtering was set at 2 Hz, low-pass filtering was set at 100 Hz, and the noise filter was also switched on. The voltages at the 3 sites on or those closest to the initial PV-encircling ablation line were retrospectively measured and averaged for analysis after the procedure (Figure S1).

2.3 | Ablation procedure

Point-by-point PVI was performed with a 3.5-mm open-irrigated-tip CF-sensing catheter (TactiCath Sensor Enabled; Abbott) with the following settings: power set to 30-40 W, target CF >5 g, target LSI >4 and interlesion distance of 4 mm with a 4-mm tag. The temperature was limited to 43°C at a saline irrigation flow rate of 17-30 mL/min during ablation. The esophageal temperature (Esophastar; Japan Lifeline Co., Ltd, Japan) alarm was set at 40°C. The endpoint of the procedure was the completion of the PVI, which was verified using a circular catheter. The decision to perform additional ablation was left to the discretion of the operators, and LA posterior wall isolation was performed in 5 cases. Cavotricuspid isthmus ablation was performed when typical atrial flutter was induced by burst atrial pacing or was observed clinically.

2.4 | AutoMark setting

PVI was performed with the AutoMark system (EnSite; Abbott). The FTI and LSI were calculated only when the ablation catheter stayed within the confined area. FTI was defined as the total CF integrated over the time of RF delivery, and the LSI was derived from a mathematical expression that incorporates CF, power and duration of RF application. AutoMark settings for filter thresholds were as follows: for catheter position stability, the minimum marker time was 4 seconds, the marker spacing was 4 mm, and the away time was 5 seconds.

2.5 | Definition of insufficient ablation sites

Insufficient ablation sites (IAS) were defined as follows: (i) spontaneous reconnection site, (ii) the PV reconnection site after dormant conduction (DC) was unmasked by adenosine injection of 20 mg, and (iii) the PV-LA gap site after the initial PVI. IAS was evaluated at least

20 min after PVI. Candidate IAS sites where the interlesion distance was >6 mm between adjacent lesions were excluded from analysis, as reconnection could be due to the spatial location of lesions rather than the failure of transmural lesion formation.

2.6 | Statistical analysis

All statistical analyses were performed using JMP 14 software (SAS Institute Inc, Cary, NC, USA). The patient characteristics data are presented as the mean ± SD or median values (25th, 75th interquartile range) for continuous variables and the number and percentage of patients for dichotomous variables. The differences between two groups were analyzed using the chi-squared test, the Wilcoxon rank-sum test or the t test. The multivariate logistic regression analysis used parameters that have already been reported to have a relationship with general IAS, and the P values were less than .05 to predict IAS.

The cutoffs for the prediction of IAS were determined using receiver operating characteristic (ROC) curve analysis by optimizing the sensitivity and specificity of the parameters. The area under the curve and 95% confidence interval of the ROC curve and the power of this study were calculated using EZR[9] (Saitama Medical Center, Jichi Medical University, Saitama, Japan), which is a graphical user interface for R (The R Foundation for Statistical Computing, Vienna, Austria). The level of statistical significance was set at $P < .05$.

3 | RESULTS

3.1 | Patient characteristics

The clinical characteristics of the 35 patients are shown in Table 1. The mean age was 67 ± 9 years, and 29 (83%) were male. Paroxysmal AF was observed in 11 (31%) patients. The average left ventricular ejection fraction and LA dimension were 60 ± 14% and 42 ± 7 mm, respectively. All patients successfully achieved PVI. No major complications occurred during or after the procedure.

3.2 | Ablation-related parameters at sites with and without insufficient ablation sites

The total number of ablation points with valid LSIs was 1417 (average: 60.3 ± 15.6 ablation points per patient). IAS was observed in 25/1417 of the total ablation sites. Spontaneous PV reconnection was observed at 16 points, ATP-provoked dormant PV conduction at 1 point, and the PV-LA gap site after the initial PVI at 8 points. The distribution of the IAS across the 16 PV segments is shown in Figure 2. The bipolar voltage amplitudes on the ablation line, LSI, o-LSI, and ablation parameters of each segment are shown in Table 2. A representative LA voltage map that indicates IAS is shown in Figure 3. IAS was significantly associated with higher bipolar voltage areas (4.20 ± 2.68 vs 2.43 ± 1.93 mV, $P < .0001$) and unipolar

TABLE 1 Patient characteristics

	All (N = 35)
Clinical characteristics	
Age (years)	67 ± 9
Gender, males, n (%)	29 (83)
BMI (kg/m^2)	25 ± 3
Paroxysmal AF, n (%)	11 (31)
Hypertension, n (%)	20 (57)
Diabetes mellitus, n (%)	5 (14)
Heart failure, n (%)	9 (26)
Stroke, n (%)	2 (6)
CHA$_2$DS$_2$VASc score	2 [1, 2]
Medication	
ACEI or ARB, n (%)	17 (49)
Antiarrhythmic drug, n (%)	20 (57)
Class I, n (%)	0 (0)
Class II, n (%)	18 (51)
Class III, n (%)	2 (6)
Class IV, n (%)	6 (17)
Laboratory data	
BNP (pg/mL)	141 [73, 241]
HANP (pg/mL)	86 [52, 164]
Ccr (mL/min)	63 [51, 72]
Echocardiographic parameter	
LVEF (%)	60 ± 14
LAD (mm)	42 ± 7

Note: Data presented as the mean $\pm$ SD, median (25th, 75th interquartile range), or n (%).

Abbreviations: ACEI, angiotensin-converting-enzyme inhibitor; AF, atrial fibrillation; ARB, angiotensin II receptor blocker; BMI, body mass index; BNP, brain natriuretic peptide; Ccr, creatinine Clearance; HANP, human atrial natriuretic peptide; LAD, left atrial dimension; LVEF, left ventricular ejection fraction.

voltage areas (2.83 ± 1.61 vs 1.90 ± 1.22 mV, $P < .001$) but not with LSI (4.5 [4.0, 4.8] vs 4.6 [4.2, 5.1], $P = .067$), FTI (144 [93, 190] vs 142 [100, 204], $P = .713$), CF (10.2 ± 4.2 vs 12.5 ± 6.4, $P = .070$), ablation time (15.3 ± 7.6 vs 14.0 ± 7.3 seconds, $P = .350$), or power (35.4 ± 4.5 vs 34.9 ± 3.5 watts, $P = .530$). The o-LSI was significantly lower at IAS than at other sites (1.14 [0.82, 1.81] vs 2.35 [1.31, 4.80] LSI/mV, $P < .0001$) (Table 3). The multivariate analysis, including the significant ablation parameters for the prediction of IAS, is shown in Table 4. The o-LSI was an independent predictor of IAS.

3.3 | Prognostic performance of o-LSI for insufficient ablation sites

The ROC curves for the prediction of IAS are shown in Figure 4. The AUC of the o-LSI (AUC of 0.742, 95% CI 0.656-0.827) was better than that of the bipolar voltage (AUC of 0.718, 95% CI 0.632-0.805). The best cutoff value for predicting IAS was 2.04 for the o-LSI (88% sensitivity and 55% specificity, $P < .0001$) and 1.84 for the bipolar voltage (92% sensitivity and 49% specificity, $P < .0001$). The prognostic performance of the o-LSI was better than that of the bipolar voltage ($P = .043$).

4 | DISCUSSION

4.1 | Main finding

The present study demonstrates that IAS was significantly associated with higher bipolar voltage areas (4.20 ± 2.68 vs 2.43 ± 1.93 mV) but not with LSI (4.5 [4.0, 4.8] vs 4.6 [4.2, 5.1]), FTI, CF, ablation time, or power. Low o-LSI, calculated as LSI/bipolar voltage, was strongly associated with IAS (1.14 [0.82, 1.81] vs 2.35 [1.31, 4.80] LSI/mV), and an o-LSI cutoff of 2.04 predicted IAS with 88% sensitivity and 55% specificity and an area under the curve of 0.74.

FIGURE 2 The distribution of the IAS across the 16 PV segments on the PVI lines. The black concentric circles indicate spontaneous reconnection, the black circles indicate dormant conduction provoked by adenosine, and the white circles indicate the PV-LA gap site after the initial PVI. LIPV, left inferior pulmonary vein; LSPV, left superior pulmonary vein; RIPV, right superior pulmonary vein; RSPV, right superior pulmonary vein
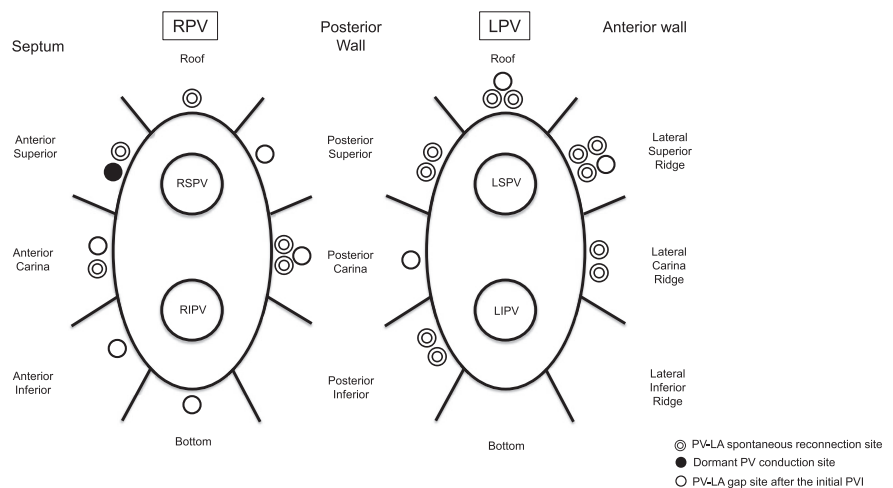
TABLE 2 Ablation parameters for each segment under the ablation line of the 16 PV-LA segments

	With IAS (n = 25)				Without IAS (n = 1392)			
	Points (n = 25)	Bipolar voltage (mV)	LSI	o-LSI	Points (n = 1392)	Bipolar voltage (mV)	LSI	o-LSI
LSPV								
Roof	3	3.32 ± 1.28	3.7 [3.3, 4.3]	1.02 [0.85, 1.99]	154	2.54 ± 1.83	4.6 [4.1, 5.0]	2.13 [1.26, 4.01]
Anterior	4	6.20 ± 2.58	4.5 [4.4, 4.9]	0.68 [0.56, 1.49]	92	2.91 ± 2.21	4.8 [4.2, 5.1]	1.91 [1.16, 3.53]
Posterior	2	2.37 ± 0.74	5.0 [4.7, 5.2]	2.18 [1.80, 2.55]	66	2.74 ± 2.05	4.4 [4.2, 4.9]	2.01 [1.15, 4.30]
LPV carina								
Anterior	2	5.67 ± 4.70	4.4 [3.6, 5.1]	1.05 [0.57, 1.53]	77	2.81 ± 2.30	4.8 [4.3, 5.1]	1.96 [1.14, 4.67]
Posterior	1	4.12	4.5	1.09	80	2.74 ± 2.22	4.3 [3.9, 4.6]	2.02 [1.15, 4.30]
LIPV								
Anterior	0	-	-	-	74	2.67 ± 2.28	4.8 [4.1, 5.1]	2.01 [1.13, 5.53]
Posterior	2	1.49 ± 0.64	3.7 [3.4, 3.9]	2.75 [1.75, 3.76]	52	2.16 ± 2.14	4.2 [3.9, 4.6]	2.44 [1.31, 5.40]
Bottom	0	-	-	-	87	2.29 ± 1.84	4.6 [4.1, 5.0]	2.44 [1.31, 5.40]
RSPV								
Roof	1	11.05	4.1	0.37	124	2.08 ± 1.73	4.7 [4.1, 5.1]	2.91 [1.45, 5.91]
Anterior	2	2.21 ± 1.67	3.7 [2.8, 4.6]	2.65 [0.82, 4.47]	76	1.81 ± 1.52	4.5 [4.1, 5.1]	3.29 [1.92, 7.73]
Posterior	1	4.87	4.7	0.97	69	2.30 ± 1.70	4.7 [4.3, 5.2]	2.28 [1.30, 5.90]
RPV carina								
Anterior	2	3.28 ± 1.30	4.6 [4.3, 4.8]	1.48 [1.14, 1.82]	86	2.43 ± 1.93	4.8 [4.2, 5.1]	2.47 [1.34, 6.66]
Posterior	3	3.38 ± 0.94	4.2 [4.1, 5.2]	1.60 [0.95, 1.66]	99	2.70 ± 1.97	4.6 [4.2, 5.0]	2.29 [1.30, 5.91]
RIPV								
Anterior	1	7.76	4.5	0.58	67	2.10 ± 1.68	5.0 [4.4, 5.2]	2.55 [1.70, 4.75]
Posterior	0	-	-	-	78	2.35 ± 1.65	4.5 [4.2, 5.0]	2.15 [1.40, 4.38]
Bottom	1	2.35	4.8	2.04	111	2.28 ± 1.55	4.8 [4.2, 5.2]	2.49 [1.44, 4.53]

Note: Data presented as the mean ± SD, median (25th, 75th interquartile range).

Abbreviations: IAS, insufficient ablation; LIPV, left inferior pulmonary vein; LSI, lesion size index; LSPV, left superior pulmonary vein; o-LSI, optimized-LSI (LSI/bipolar voltage); RIPV, right inferior pulmonary vein; RSPV, right superior pulmonary vein.
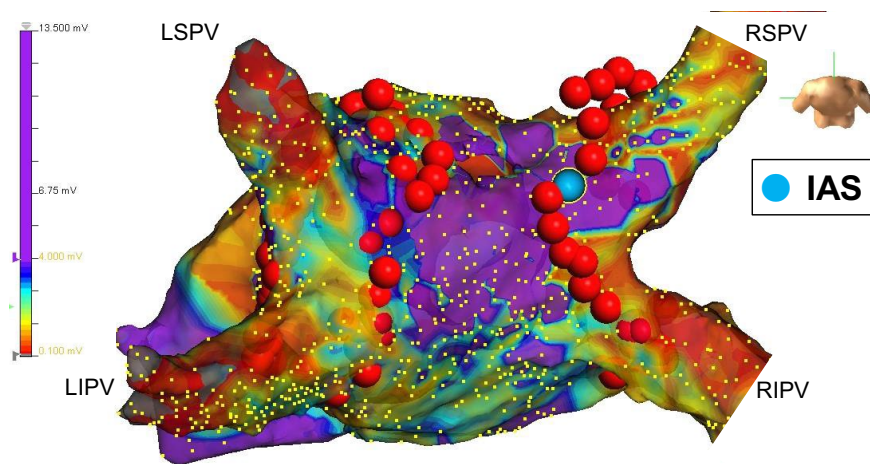

FIGURE 3 A representative PV-LA bipolar voltage map. The purple areas are defined as high-voltage areas (>4.00 mV), and the blue, green, yellow, orange, and red areas are low-voltage areas (<4.00 mV). In this case, an IAS was observed in a relatively high-voltage area, which was at the superior posterior aspect of the RSPV. IAS, insufficient ablation sites; LIPV, left inferior pulmonary vein; LSPV, left superior pulmonary vein; RIPV, right superior pulmonary vein; RSPV, right superior pulmonary vein

TABLE 3 Ablation-related parameters with and without insufficient ablation sites

	All (n = 1417)	With IAS (n = 25)	Without IAS (n = 1392)	P value
Bipolar voltage on the PVI line (mV)	2.46 ± 1.95	4.20 ± 2.68	2.43 ± 1.93	<.0001
Unipolar voltage on the PVI line (mV)	1.92 ± 1.23	2.83 ± 1.61	1.90 ± 1.22	<.001
Mean RF duration (sec)	14.0 ± 7.3	15.3 ± 7.6	14.0 ± 7.3	.350
Mean RF temperature (℃)	36.1 ± 2.1	35.5 ± 2.0	36.1 ± 2.0	.181
Mean RF power (W)	34.9 ± 3.5	35.4 ± 4.5	34.9 ± 3.5	.530
Mean contact force (g)	12.5 ± 6.4	10.2 ± 4.2	12.5 ± 6.4	.070
Mean impedance drop (Ω)	15.9 ± 6.3	14.7 ± 4.5	16.0 ± 6.4	.335
FTI (gs)	142 [100, 203]	144 [93, 190]	142 [100, 204]	.713
LSI	4.6 [4.2, 5.1]	4.5 [4.0, 4.8]	4.6 [4.2, 5.1]	.067
o-LSI (LSI/bipolar voltage)	2.28 [1.31, 4.72]	1.14 [0.82, 1.81]	2.35 [1.31, 4.80]	<.0001

Note: Data presented as the mean ± SD, median (25th, 75th interquartile range).

P values are for the with IAS group vs without IAS group.

Abbreviations: FTI, force time integral; IAS, insufficient ablation sites; LSI, lesion size index; o-LSI, optimized-LSI (LSI/bipolar voltage); PVI, pulmonary vein isolation; RF, radiofrequency.

TABLE 4 Multivariate analysis including the significant parameters for the prediction of insufficient ablation sites

	Multivariate analysis		
	Odds ratio	95% CI	P value
Mean contact force (g)	0.95	0.845-1.044	.303
FTI (gs)	1.00	0.996-1.010	.330
LSI	0.51	0.210-1.330	.166
o-LSI (LSI/bipolar voltage)	0.54	0.328-0.777	<.001

Abbreviations: CI, confidence interval; FTI, force time integral; LSI, lesion size index; o-LSI, optimized-LSI (LSI/bipolar voltage); PVI, pulmonary vein isolation; RF, radiofrequency.

4.2 | LSI-guided PVI

PVI is the most important and effective strategy for AF ablation,[10] and the creation of durable ablation lesions is essential to achieve permanent isolation of PV. However, as previously demonstrated, a large number of AF recurrences are still due to reconnected PV.[11-13]

Recently, the EnSite NavX CF module with LSI was developed to allow better standardization of ablation lesion size. LSI, which is an index calculated from power, time, and CF, has been reported to be superior for predicting lesion size than FTI, and LSI-guided PVI can provide stable RF application without an increase in the complication rate compared with standard, non-LSI-guided approaches. Kanamori et al reported that the optimal LSI threshold for predicting gaps or DCs was 4.05 (sensitivity, 63.4%; specificity, 76.3%), and

an LSI of <5.25 highly predicted gap or DC formation (sensitivity, 97.6%; specificity, 25.7%).[14]

However, data are still limited for the optimal LSI target for PVI, and it is sometimes difficult to achieve first-pass PVI and to avoid acute PV reconnections even with the LSI-guided procedure. The reason IAS is still observed might be due to the characteristics of atrial tissue.

4.3 | Atrial voltage mapping with the Advisor™ HD Grid catheter and atrial tissue characteristics

Noninvasive modalities such as CT and magnetic resonance imaging (MRI) are effective in detecting the wall thickness or the area of scarring, and the regions with reduced bipolar voltage are correlated with fibrotic tissue on MRI.[15] However, it is difficult to incorporate the information of such noninvasive modalities into the real-time 3D mapping system. Multipolar mapping catheters, such as multielectrode circular mapping catheters (CMCs), have been used for voltage mapping for the purpose of creating an HD map, although it is difficult to contact CMCs with the endocardium, which can result in poor signal recordings, and the bipolar voltage generated by a specific-direction bipolar pair of CMCs can be greatly affected by the local propagation direction. The recently released Advisor™ HD Grid catheter features a HD rectangular-shaped grid that is designed to achieve better electrode–tissue contact than CMCs. It can record the highest amplitude bipolar voltage among 32 bipolar signals (16 along the splines and 16 across the splines), which is independent of propagation direction.[16] Based on this structural feature, the Advisor™ HD Grid catheter is expected to provide more accurate information about the area
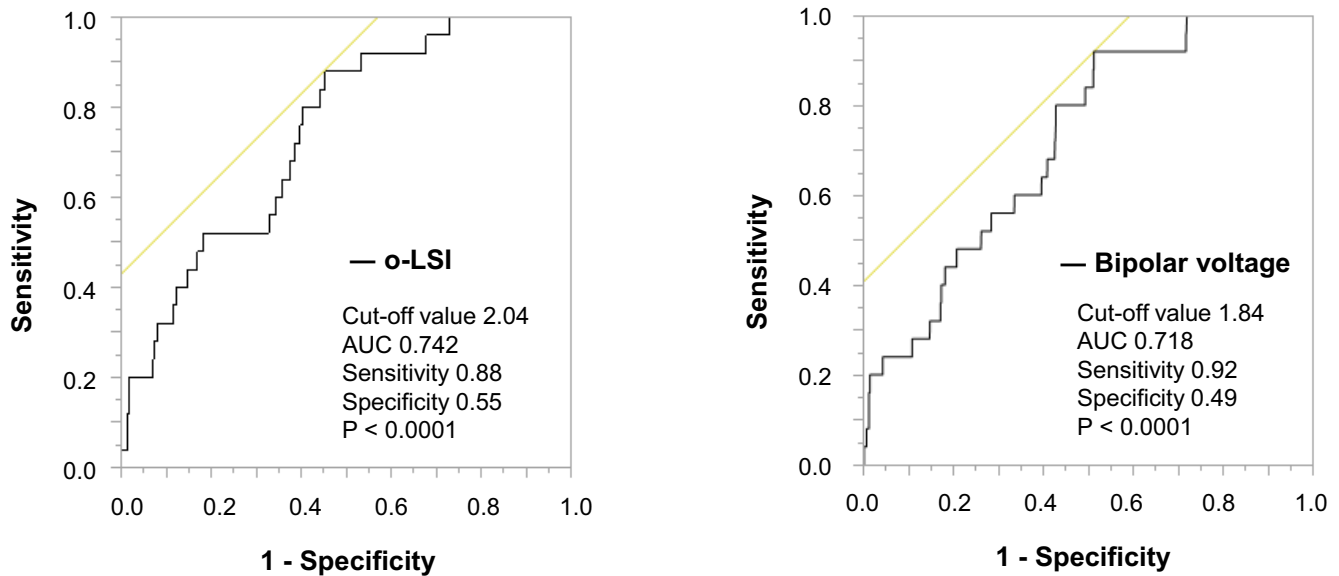
	Cut-off value	Sensitivity	Specificity	AUC (95% CI)	*P Value*
o-LSI (LSI/Bipolar voltage)	2.04	0.88	0.55	0.742 (0.656-0.827)	0.043
Bipolar voltage on the PVI line (mV)	1.84	0.92	0.49	0.718 (0.632-0.805)	

AUC = area under the curve, CI = confidence interval, o-LSI = optimized Lesion size index, PVI = Pulmonary vein isolation.

FIGURE 4 The ROC curves for the prediction of IAS are shown in Figure 4. The AUC of the o-LSI (AUC of 0.742, 95% CI 0.656-0.827) was better than that of the bipolar voltage (AUC of 0.718, 95% CI 0.632-0.805). The best cutoff value for predicting IAS was 2.04 for the o-LSI (88% sensitivity and 55% specificity, *P* < .0001) and 1.84 for the bipolar voltage (92% sensitivity and 49% specificity, *P* < .0001). The prognostic performance of the o-LSI was better than that of the bipolar voltage (*P* = .043). ROC, receiver operating characteristic; IAS, insufficient ablation sites; AUC, area under the curve; o-LSI, optimized lesion size index (LSI/bipolar voltage)

of scar or low-voltage areas. Nagashima et al reported that the PV-LA voltage was a simple real-time variable obtained at sites accurately mapped in a 3D mapping system, and the high PV-LA voltage on the PV-encircling ablation line was related to acute post-PVI PV reconnections; nevertheless, the voltage amplitudes correlated weakly with the PV-LA junction wall thicknesses.[7] This result suggested that the voltage amplitudes could reflect the nature of the atrial tissue and should be applied to the ablation procedure because the atrial tissue wall thickness and the characteristics of the tissue, such as whether it is diseased or healthy, are different at every ablation point.

4.4 | Combination of LSI and bipolar voltage within the PV-encircling lines

We defined the o-LSI, calculated as LSI/bipolar voltage, as a combination with two parameters. The sensitivity for the IAS of o-LSI was high, but the specificity was low (88% sensitivity and 55% specificity). This result indicates that it is not always necessary to ablate with a high LSI in the HVZ, but additional ablation is sometimes required in the HVZ when IAS is observed. When PVI is not achieved after performing initial encircling ablation at the PV-LA antrum, low o-LSI values could provide a clue to the locations requiring additional

ablation. Furthermore, o-LSI might enable judicious adjustment of energy delivery based on the properties of the atrial substrate to adequately address thicker myocardial tissue in higher-voltage zones while avoiding complications at sites with thinner myocardium or atrial scarring due to unnecessary ablation. o-LSI-guided PVI has the potential to achieve necessary and sufficient RF applications. Future prospective studies will be required to determine whether the o-LSI-guided ablation strategy can improve AF ablation outcomes.

5 | STUDY LIMITATIONS

Our study has several limitations. First, this study was a single-center retrospective study with a relatively small sample size; therefore, selection bias and unmeasured confounders could not be excluded. Second, IAS might be caused by multiple other factors, such as catheter contact angle, stability, or blood flow and trabecula in the LA. Third, at the anterior portion of the left-sided PV, the local electrogram of the PV generally overlaps with that of the left atrial appendage. Since we evaluated the highest bipolar voltage acquired by the Advisor™ HD Grid catheter, it was impossible to distinguish between those electrograms. Fourth, the optimal cutoff value of the o-LSI should be validated using different populations. Finally, IAS

was evaluated only in the acute phase, and data from the chronic phase are lacking. Long-term reexamination of IAS is needed to improve the ablation procedure.

6 | CONCLUSION

A low level of o-LSI was strongly associated with IAS. The combination of LSI and bipolar voltage within the PV-encircling lines may potentially provide novel strategies for durable PVI.

CONFLICTS OF INTEREST
This study received no financial support from commercial sources, and the authors have no conflicts of interest to declare.

ORCID
Gen Matsuura (ID) https://orcid.org/0000-0003-0165-5677
Jun Kishihara (ID) https://orcid.org/0000-0002-5920-4417
Hidehira Fukaya (ID) https://orcid.org/0000-0002-7588-554X
Ryo Nishinarita (ID) https://orcid.org/0000-0003-0329-5476
Shinichi Niwano (ID) https://orcid.org/0000-0002-0702-0800

REFERENCES
1. Parkash R, Tang AS, Sapp JL, Wells G. Approach to the catheter ablation technique of paroxysmal and persistent atrial fibrillation: a meta-analysis of the randomized controlled trials. J Cardiovasc Electrophysiol. 2011;22:729–38.
2. Calkins H, Hindricks G, Cappato R, et al. 2017 HRS/EHRA/ECAS/APHRS/SOLAECE expert consensus statement on catheter and surgical ablation of atrial fibrillation: executive summary. Europace. 2018;20:157–208.
3. Ouyang F, Tilz R, Chun J, Schmidt B, Wissner E, Zerm T, et al. Long-term results of catheter ablation in paroxysmal atrial fibrillation: lessons from a 5-year follow-up. Circulation. 2010;122:2368–77.
4. Calzolari V, De Mattia L, Indiani S, et al. In vitro validation of the lesion size index to predict lesion width and depth after irrigated radiofrequency ablation in a porcine model. JACC Clin Electrophysiol. 2017;3:1126–35.
5. Lambert H, Olstad SJ, Fremont OB. Prediction of atrial wall electrical reconnection based on contact force measured during RF ablation. United States Patent Application Publication. Pub. No. US 2012/0209260 A1. August 16.
6. Mattia L, Crosato M, Indiani S, et al. Prospective evaluation of lesion index-guided pulmonary vein isolation technique in patients with paroxysmal atrial fibrillation: 1-year follow-up. J Atr Fibrillation. 2018;10:1858.
7. Nagashima K, Watanabe I, Okumura Y, Iso K, Takahashi K, Watanabe R, et al. High-voltage zones within the pulmonary vein antra: major determinants of acute pulmonary vein reconnections after atrial fibrillation ablation. J Interv Card Electrophysiol. 2017;49:137–45.
8. Takahashi K, Okumura Y, Watanabe I, Nagashima K, Sonoda K, Sasaki N, et al. Relation between left atrial wall thickness in patients with atrial fibrillation and intracardiac electrogram characteristics and ATP-provoked dormant pulmonary vein conduction. J Cardiovasc Electrophysiol. 2015;26:597–605.
9. Kanda Y. Investigation of the freely available easy-to-use software 'EZR' for medical statistics. Bone Marrow Transplant. 2013;48:452–8.
10. Martins RP, Galand V, Behar N, Daubert J-C, Mabo P, Leclercq C, et al. Localization of residual conduction gaps after wide antral circumferential ablation of pulmonary veins. JACC Clin Electrophysiol. 2019;5:753–65.
11. Ouyang F, Ernst S, Chun J, Bänsch D, Li Y, Schaumann A, et al. Electrophysiological findings during ablation of persistent atrial fibrillation with electroanatomic mapping and double Lasso catheter technique. Circulation. 2005;112:3038–48.
12. Nery PB, Belliveau D, Nair GM, et al. Relationship between pulmonary vein reconnection and atrial fibrillation recurrence: a systematic review and meta-analysis. JACC Clin Electrophysiol. 2016;2:474–83.
13. Verma A, Kilicaslan F, Pisano E, Marrouche NF, Fanelli R, Brachmann J, et al. Response of atrial fibrillation to pulmonary vein antrum isolation is directly related to resumption and delay of pulmonary vein conduction. Circulation. 2005;112:627–35.
14. Kanamori N, Kato T, Sakagami S, Saeki T, Kato C, Kawai K, et al. Optimal lesion size index to prevent conduction gap during pulmonary vein isolation. J Cardiovasc Electrophysiol. 2018;29:1616–23.
15. Oakes RS, Badger TJ, Kholmovski EG, Akoum N, Burgon NS, Fish EN, et al. Detection and quantification of left atrial structural remodeling with delayed-enhancement magnetic resonance imaging in patients with atrial fibrillation. Circulation. 2009;119:1758–67.
16. Masuda M, Asai M, Iida O, Okamoto S, Ishihara T, Nanto K, et al. Left atrial voltage mapping with a direction-independent grid catheter: comparison with a conventional circular mapping catheter. J Cardiovasc Electrophysiol. 2019;30:2834–40.

SUPPORTING INFORMATION
Additional supporting information may be found online in the Supporting Information section.